

Transport properties of RTILs from classical molecular dynamics

Oliviero Andreussi^{1,2,*} and Nicola Marzari^{2,†}

¹*Massachusetts Institute of Technology,
Department of Material Science and Engineering,
77 Massachusetts Ave. Cambridge 02139 MA, USA*

²*Theory and Simulations of Materials,
École Polytechnique Fédérale de Lausanne,
Station 12, 1015 Lausanne, Switzerland*

Abstract

Room Temperature Ionic Liquids (RTILs) have attracted much attention in the scientific community in the past decade due to their novel and highly customizable properties. Nonetheless their high viscosities pose serious limitations to the use of RTILs in practical applications. To elucidate some of the physical aspects behind transport properties of RTILs, extensive classical molecular dynamics (MD) calculations are reported. Bulk viscosities and ionic conductivities of butyl-methyl-imidazole based RTILs are presented over a wide range of temperatures. The dependence of the properties of the liquids on simulation parameters, e.g. system size effects and choice of the interaction potential, is analyzed.

* oliviero.andreussi@epfl.ch

† nicola.marzari@epfl.ch

I. INTRODUCTION

In recent years, room temperature ionic liquids (RTILs) have seen much interest due to their promising properties in “green chemistry” applications [1]. Similarly to the well known high temperature molten salts, RTILs are liquids composed solely by ions. As opposite to molten salts, the presence of large asymmetric organic cations inhibits crystallization and allows these salts to be liquid at temperature as low as 100°C. Despite the fact that the first report of a RTIL dates back to the beginning of the last century [2], the first generation of RTILs, based on chloroaluminate(III) systems, was theoretically predicted [3] and experimentally realized [4, 5] just in the 1980’s. Nonetheless, practical applications of chloroaluminate ionic liquids were strongly limited by their high moisture sensitivity [6, 7]. It is just with the advent of water and air stable RTILs [8] that the full potential of these new compounds became apparent. Several reviews on this topic appeared in the last years [1, 9–14], clearly highlighting the interest in this field .

Properties of RTILs are as different from standard molecular solvents as ionic crystals differ from molecular ones. Due to the ionic nature of their constituents, RTILs generally show negligible vapor pressure and high thermal stability, and they tend to be very good solvent for most organic and inorganic species. Moreover, they typically present very high electrochemical stability and are intrinsically able to conduct electrical currents. Despite all these remarkable properties, none of the existing RTILs possess all of them at the same time. Nonetheless, since RTILs are based on organic molecules, they can be easily modified by standard chemical reactions. Indeed, both the cation and the anion can be individually modified in order to tune the physico-chemical properties of the resulting RTIL. This allows a great degree of flexibility in the design of the most suitable compound, given that the number of different possible combinations scales as the product of the number of oppositely charged ions. When considering the number of binary and ternary mixtures of all available cations and anions, the range of possibilities quickly diverges. In this perspective, the idea of task-specific RTILs has emerged and applications of RTILs in the most diverse fields have been proposed, and patented. Organic synthesis and catalysis, extraction, and treatment of rare-earth elements are some of the most studied fields of application of RTILs.

Particular attention has been devoted to the possible applications of RTILs in electrochemistry [13]. Specifically, RTILs as electrolytes in dye-sensitized solar cells [15–17], fuel

cells[18], and lithium batteries [19] have been extensively studied both for safety and efficiency. Indeed, the low volatility of these liquids insures their safety against combustion and explosion. On the other hand, some of the existing RTILs present very high electrochemical stability, thus allowing the use of higher voltages in batteries and improving the overall efficiency of the devices. A major limitation in actual applications of RTILs as electrolytes is represented by the high viscosities of all RTILs known to date. Even though the conductivity of some of the available RTILs is already sufficiently high for battery applications [19], design rules to improve ionic conductivity are currently the subject of intense experimental and theoretical study. In this context, much of the scientific effort is directed toward understanding of the molecular mechanisms that influence the transport properties of RTILs.

Despite the huge increase in the literature on RTILs, experimental results still suffer from some limitations, and in particular can be affected by the presence of water and impurities in the systems studied [20]. Indeed, water was shown to strongly affect transport properties of RTILs, with a decrease of diffusion coefficients by orders of magnitude in water-RTILs mixtures being reported [21]. A full quantitative characterization of the amount and kind of impurities is often lacking and results can be difficult to compare.

In order to provide a detailed picture of the molecular mechanisms behind the properties of RTILs, several theoretical works have appeared in the literature. The first semi empirical and ab-initio calculation on RTILs were performed at the end of the 1980s [3, 4], with the main purpose of investigating the stability and the structure of isolated ions; theoretical literature on RTILs started increasing after 2001, when some of the first parametrization of classical interaction potentials (force fields) were reported [22–28]. The first calculations typically also reported results on single ions and ion pairs as obtained from density-functional theory (DFT). These results were used to fit classical empirical potentials that were exploited to compute some of the fundamental properties of the liquids. In order to validate the force fields against available experimental results, radial and angular distribution functions, densities and diffusion coefficients were the first quantities investigated. The agreement between simulation results and experimental data were not always satisfactory, with some approximation in the functional form of the interaction potential being too crude [29]. In particular, it was shown that using an All Atom picture instead of a Unified Atoms Method was more effective in reproducing experimental densities [25]. Similarly, including polarization effects

was shown to significantly improve the agreement with experimental results, in particular for transport properties [30]. Despite some of the limitations of the available force fields, MD simulations were effective in predicting and validating some of the new features characteristic of the RTILs' structure, such as the presence of heterogeneities and holes in the liquids [31]. Nonetheless, some properties still lack an accurate analysis and characterization. This is particularly true for transport properties, such as viscosity and conductivity, that, due to the slow glassy-like dynamics of most RTILs, require long simulation times and large system sizes. Indeed, while parametrized force fields are generally checked against structural properties, few groups have reported careful analysis of viscosities and conductivities [32–36]. For these reasons, in the present work an extensive set of classical MD simulations on prototypical RTILs are reported. After a short methodological section (II), our results on the effect of temperature and simulation parameters on the transport properties are presented (IIIA). Eventually, results on ionic liquids based on different anions are compared in Section IIIB.

II. SIMULATION DETAILS

Classical molecular dynamics (MD), as implemented in the DL_POLY program, was used throughout [37–39]. Three different 3-butyl-1-methylimidazolium (BMIM) based RTILs were examined, namely the salts obtained with the PF_6^- , BF_4^- , and bis(trifluoromethylsulfonyl)imide (Tf_2N^-) anions. As for the interaction potential, three different force field were considered for the case of BMIM- PF_6 [23, 40–42], while simulations on BMIM- BF_4 and BMIM- Tf_2N were performed using the force fields developed by Canongia-Lopes et al. [41–43]. An interaction cutoff radius of 15 Å was used throughout. Initial configurations containing 128, 432 and 1024 ion pairs were generated starting from a fcc cubic lattice with the ions occupying random lattice sites. Equilibration in the NPT ensemble was enforced using Berendsen's thermostat and barostat [44], with equilibration runs performed until convergence of the statistical average of the density was achieved. Following equilibration, up to four different production runs for each system were performed in the NVT ensemble, using the Nose-Hoover thermostat [45, 46]. A simulation timestep of 2 fs was used for temperatures lower or equal to 500 K, while 1 fs was chosen for simulations at higher temperatures.

Diffusion coefficients of the ions were computed in terms of mean square displacements

(MSD)

$$\langle r_i^2(t) \rangle = \langle |\vec{r}_i(t) - \vec{r}_i(0)|^2 \rangle,$$

using the Einstein relation [47, 48]

$$D_i = \lim_{t \rightarrow \infty} \frac{1}{6} \frac{\partial \langle r_i^2(t) \rangle}{\partial t}. \quad (1)$$

Following standard methodology (e.g. as reported in [34]), to assess the true diffusive behavior of the ions, MSDs will be displayed in log-log plots, together with their slopes $\beta(t)$ as a function of time

$$\beta(t) = \frac{d \log MSD(t)}{d \log t}. \quad (2)$$

At very short times, a value of β equal to two is expected, corresponding to a free, ideally ballistic, motion of the ions. On the other extreme, at very long times β should reach a value equal to one, corresponding to real diffusive regime, in which the mean square displacement of the ion grows linearly with time. At intermediate times a sub-linear behavior is expected, characterized by a logarithmic slope $\beta(t)$ lower than one. We would like to stress here that this analysis is crucial in determining the effective achievement of diffusive behavior and to determine the portion of the MSD plot that should be used to fit diffusion coefficients. This is particularly important in the case of slow, viscous liquids such as RTILs.

The Einstein formalism was also used in the calculation of ionic conductivities [47, 48]

$$\lambda = \lim_{t \rightarrow \infty} \frac{e^2}{6Vk_B T} \frac{\partial \langle \sum_{i,j=1}^N z_i z_j \vec{r}_i(t) \vec{r}_j(t) \rangle}{\partial t}, \quad (3)$$

while viscosities (η) were computed from the auto correlation of the off diagonal elements of the stress tensor σ^{xy} , exploiting the Green-Kubo relation [47, 48]

$$\eta = \frac{V}{k_B T} \int_0^\infty \langle \sigma^{xy}(0) \sigma^{xy}(t) \rangle dt. \quad (4)$$

III. RESULTS

A. BMIM-PF6

A system composed of 128 BMIM-PF6 ion pairs, described with the interaction potential parametrized by Liu et al. (ref. [40], abbreviated in the following as LHW2004), was equilibrated at several temperatures, ranging from 300 K to 1000 K. Densities, reported

Systems	$\rho(\text{g/cm}^3)$	$D^+ (\text{m}^2/\text{s})$	$D^- (\text{m}^2/\text{s})$	$\eta (\text{mPas})$	$\lambda (\text{S/cm})$
298.15 K (exp [50])	1.37	$1.6 \pm 0.2 \cdot 10^{-11}$	-	196 ± 20	$4.04 \pm 0.4 \cdot 10^{-3}$
300 K (exp [49])	1.37	$8.0 \pm 3.0 \cdot 10^{-12}$	$5.9 \pm 2.4 \cdot 10^{-12}$	230 ± 65	$1.66 \pm 0.3 \cdot 10^{-3}$
300 K	1.36	$4.8 \pm 1.0 \cdot 10^{-13}$	$2.6 \pm 0.5 \cdot 10^{-13}$	2400 ± 2000	$1.5 \pm 0.7 \cdot 10^{-4}$
350 K	1.33	$4.0 \pm 1.0 \cdot 10^{-12}$	$2.0 \pm 0.8 \cdot 10^{-12}$	940 ± 400	$1.9 \pm 0.8 \cdot 10^{-3}$
375 K	1.32	$1.0 \pm 0.1 \cdot 10^{-11}$	$6.2 \pm 1.0 \cdot 10^{-12}$	421 ± 200	$1.4 \pm 0.5 \cdot 10^{-3}$
400 K	1.29	$3.1 \pm 0.1 \cdot 10^{-11}$	$2.0 \pm 0.3 \cdot 10^{-11}$	111 ± 4	$8.7 \pm 0.6 \cdot 10^{-3}$
450 K	1.26	$1.14 \pm 0.06 \cdot 10^{-10}$	$7.9 \pm 0.8 \cdot 10^{-11}$	31 ± 1	$1.5 \pm 0.3 \cdot 10^{-2}$
500 K	1.22	$2.5 \pm 0.2 \cdot 10^{-10}$	$1.9 \pm 0.1 \cdot 10^{-10}$	12 ± 1	$4.8 \pm 1.0 \cdot 10^{-2}$
600 K	1.16	$8.5 \pm 0.1 \cdot 10^{-10}$	$7.5 \pm 0.04 \cdot 10^{-10}$	7 ± 1	$9.7 \pm 1.0 \cdot 10^{-2}$
1000 K	0.87	$7.6 \cdot 10^{-9}$	$7.3 \cdot 10^{-9}$	5	$2.25 \cdot 10^{-1}$

Table I. Densities ρ , cation diffusion coefficients D^+ , anion diffusion coefficients D^- , viscosities η , and conductivities λ of the BMIM-PF6 RTIL as a function of temperature, as computed by classical NVT molecular dynamics simulations on a periodic cell of 128 ion pairs using the LHW2004 force field.

in Table I, are in agreement with what reported in the literature and show a good match with the experimental results [49, 50] available at the lowest temperatures. The radial distribution functions of the system (reported in Figure 1) are also in very good agreement with previous results [40]. In order to provide a more detailed description of the structure of the liquid, when analyzing radial distributions the cation has been subdivided in two distinct regions, corresponding to the charged aromatic ring (R) and the long alkylic tail (T). Charge-induced correlations in the liquid can be clearly evinced from the reported plots and persist, with some broadening, even at the highest temperatures considered. Van der Waals interactions, instead, are responsible for the high degree of correlation between the alkyl chains of the cations. Due to the local, short-range nature of the Van der Waals interaction, the first peak in the tail-tail plot is one of the most sensible to temperature, shifting towards larger distances as the simulation temperature increases.

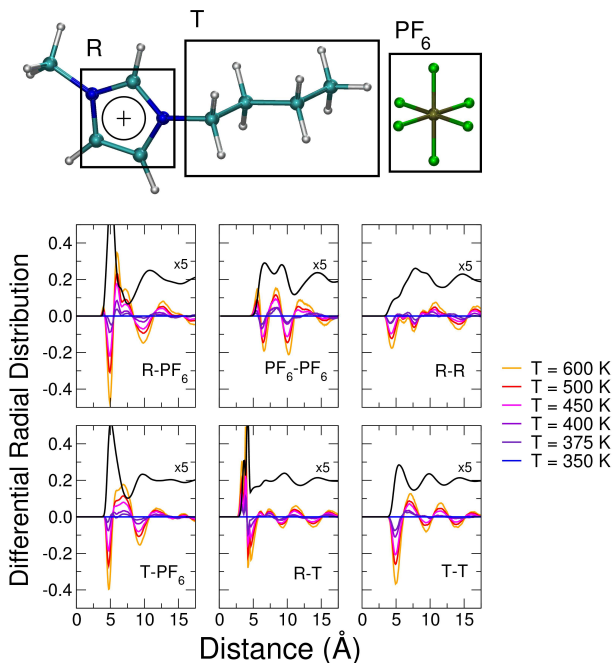


Figure 1. Radial distribution functions of BMIM-PF₆ RTIL, as computed by classical NVT molecular dynamics simulations on a periodic cell of 128 ion pairs described by the LHW2004 force field. The BMIM cation (top panel) is partitioned in two distinct subregions, corresponding to the charged aromatic ring (R) and the long alkylic tail (T). The radial distribution functions at 300 K are reported in black, while for higher temperatures the differentials radial distributions with respect to 300 K have been reported (colored lines). Strong charge induced correlations are evident from the leftmost series of panels. A reasonably strong correlation is also present between the alkyl tails of the cation, as shown in the T-T plot (rightmost series, central panel). All the distribution functions show non-negligible correlations for distances as long as half the cell size, even at the highest temperatures.

1. Transport Properties

Mean square displacements of the different ions are reported in Figure 2 as a function of time, for the range of temperatures studied.

Despite the remaining noise in the logarithmic derivatives at long times, it is seen from these plots that a diffusive behavior is reached within the simulation times at each temperature but the lowest one. Diffusion times, i.e. the times necessary to the ions to reach a

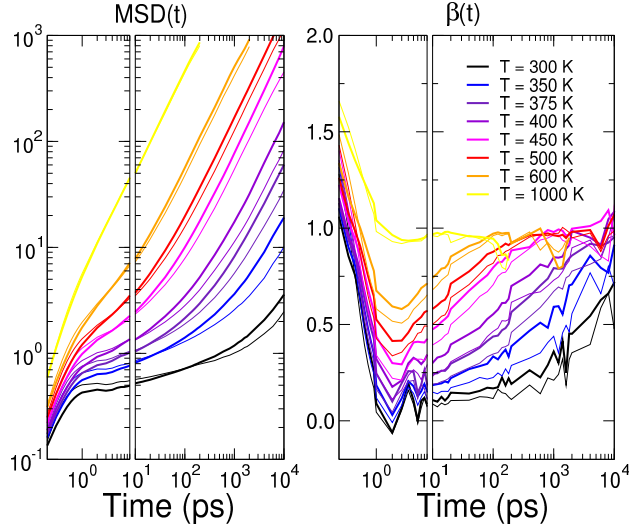


Figure 2. Mean square displacements (left panel) and corresponding values of β (Eq. 2) for the BMIM-PF₆ RTIL, as computed by classical NVT molecular dynamics simulations on a periodic cell of 128 ion pairs described by the LHW2004 force field. Cations are represented by thick lines, while thin lines are used for the anions. In order to characterize MSDs at short times, a separate set of simulations was used, characterized by a very short (0.5ps) time between sampling different configurations.

diffusive regime with $\beta \simeq 1$, are summarized in Figure 3. The curves show a divergent behavior at low temperature and can be fitted with good accuracy by a Vogel-Fulcher-Tammann relation $f = A \exp(B/(T - T_0))$. A value of $B \simeq 1720/1730$ and a divergence temperature $T_0 \simeq 200/215$ K can be extracted for the diffusion times of the cation and the anion respectively. By extrapolating these behavior to the lowest temperature considered (300 K), a diffusion time of the order of 10^8 ps can be estimated. Thus, a straightforward determination of the diffusion coefficients of the ions at this temperature appears beyond the limits of standard computational resources. For this reason, the different transport properties of the system at 300 K are only estimated by averaging the results over several independent calculations. In order to improve the statistics in the results and get an estimate of the errors, the same approach was used for simulations below 600 K, that show diffusion times of the order of few nanoseconds.

Diffusion coefficients of both the cations and the anions, reported in Figure 4 and in Table I, show Arrhenius behavior at high temperatures, while a deviation from linearity is evident

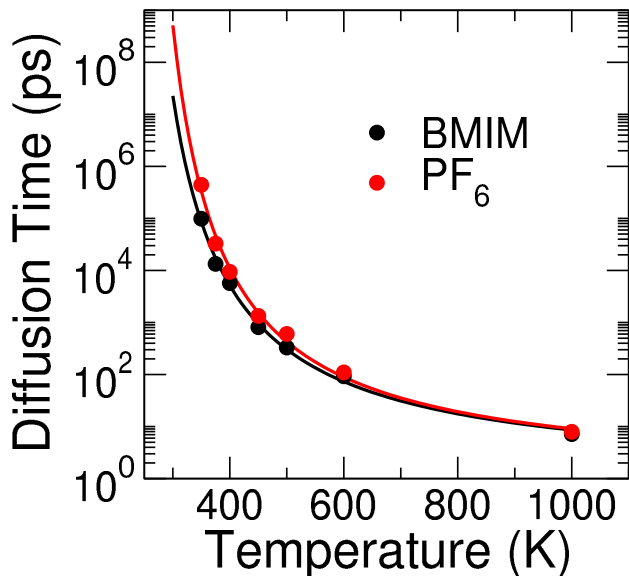


Figure 3. Diffusion times, i.e. times necessary to the ions to reach a diffusive regime with $\beta \simeq 1$, as extracted from classical NVT molecular dynamics simulations on a periodic cell of 128 BMIM-PF₆ ion pairs, as described by the LHW2004 force field (filled circles). Non-linear curve fits of the form $f = A \exp(B/(T - T_0))$ are added to the computed results and represented with solid lines.

at the lowest temperatures. As expected, diffusion coefficients at 300K appear overestimated, due to the lack of a true diffusive regime in the simulations at this temperature. Activation energies of $E = 31.4/28.4 \cdot 10^{-3} \text{kJ/mol}$ for the diffusion of the cation/anion can be inferred from the high temperature slopes of the curves reported in Figure 4. The change in slope at low temperature is an indication of the glassy behavior of the liquid, consistent with the very slow non-ergodic dynamics of the systems in this range of temperatures. As was done for the diffusion times, fitting the data with a Vogel-Fulcher-Tammann relation points to a divergence temperature $T_0 \simeq 230/235 \text{ K}$. The correct qualitative behavior of the results is well reproduced, together with accurate slopes as a function of temperature, with anions diffusing slower than cations, despite their smaller size. The higher conformational flexibility of the cation, due to the presence of alkyl chains, is generally acknowledged as the main explanation for this behavior. Nonetheless, computed results are one order of magnitude far from the experimental data available at the lowest temperatures [49]. This discrepancy may be due to the intrinsic deficiency of the non polarizable force-field to reproduce the real dynamics of the systems [30]. On the other hand, the presence of even a small fraction of impurities in the experimental samples can be responsible for a significant change in the

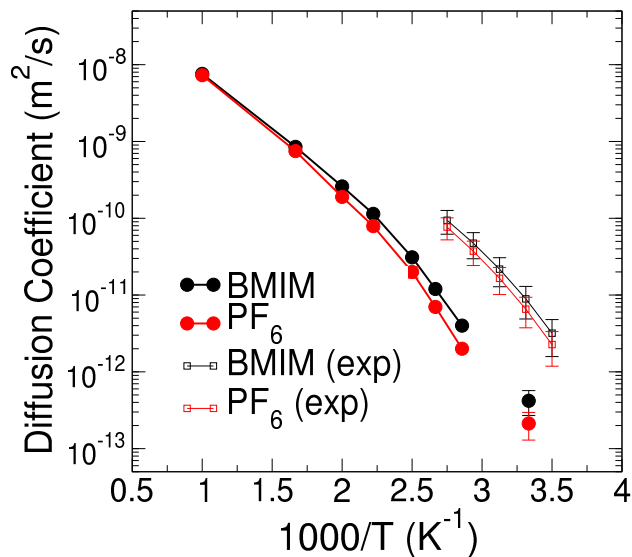


Figure 4. Diffusion coefficients of cations (black) and anions (red) as extracted from the MSDs computed on a periodic cell of 128 BMIM-PF₆ ion pairs, as described by the LHW2004 force field (filled circles). Experimental results from Ref. [49] are also reported for comparison (empty squares).

reported results [21].

It is important to note that original results on the LHW2004 force field [40] showed an impressive agreement with experiments. This apparent contradiction can be explained by the very short simulation times used to extrapolate the diffusion coefficients in Ref. [40]. Especially for results at the lowest temperature, according to the considerations above and the results in Figure 3, a sub-linear non-diffusive behavior of the MSD should be inferred for all simulation times reported in Ref. [40]. Longer simulations on the same systems at 350 K appeared in the literature [51] and showed a remarkable agreement with the present results, thus validating our conclusions.

Viscosities and ionic conductivities of the system are reported in Figure 5 and summarized in Table I. As for the case of diffusion coefficients, also viscosities and conductivities show significant deviations from experimental results. In both cases, results one order of magnitude lower than the values reported in the literature were obtained, even if their trends with respect to temperature are also well reproduced. It should be stressed that the uncertainties in the computed values for these quantities are higher than the average errors in computing diffusion coefficients: this is due to the fact that viscosity and conductivity are global prop-

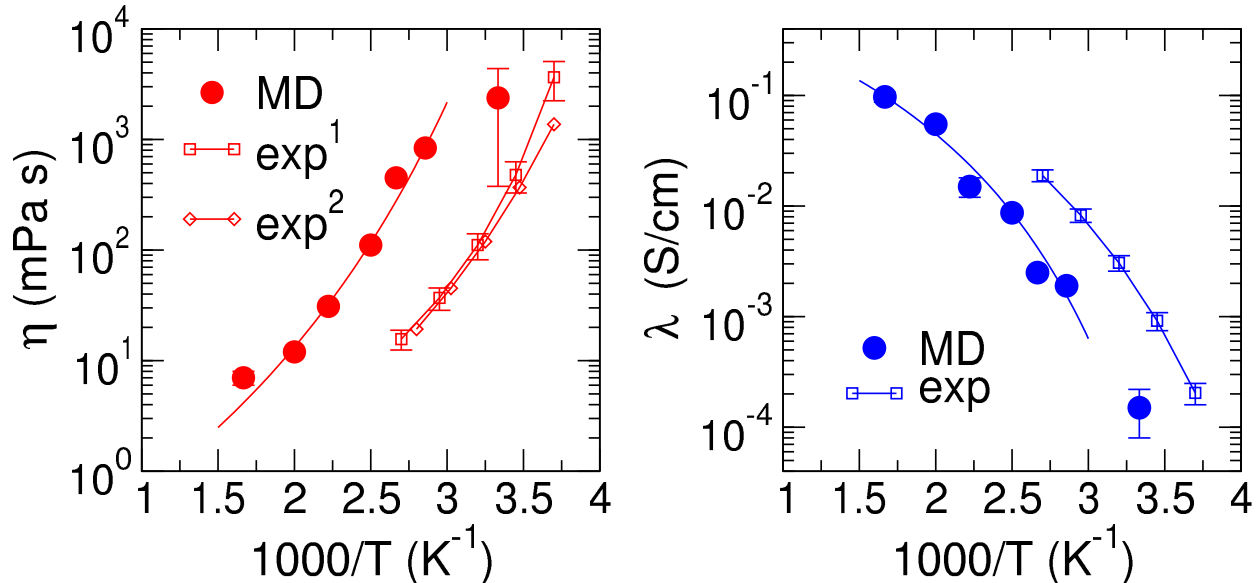


Figure 5. Bulk viscosities (left) and ionic conductivities (right) of BMIM-PF6, as computed by classical NVT molecular dynamics simulations on a periodic cell of 128 ion pairs described by the LHW2004 force field. Experimental results from Ref.[49](exp^1 , empty squares) and Ref.[50] (exp^2 , empty diamonds) are also reported for comparison.

erties of the system, while diffusion coefficients calculations benefit from ensemble averages over all different particles in the system.

2. Size effects

As shown by the radial distribution functions (Figure 1), Coulomb-induced ordering of the systems is significant for distances comparable and larger than the 128 ion pairs simulation cell. Thus, particular care should be taken in evaluating size effects on the structure and on the transport properties of the liquid.

In Figure 6 the radial distribution functions as a function of the number of ion pairs (128, 432, 1024) are reported at 400 K. Correlations due to the electrostatic interactions in the liquid decay completely at half the cell size only for the larger systems, composed by 1024 ion pairs. Nonetheless, the local structure of the liquid is well reproduced in the smaller systems, the differences in the computed radial distribution functions being generally less than 2%.

In agreement with what was found for the distribution functions, results in Table II

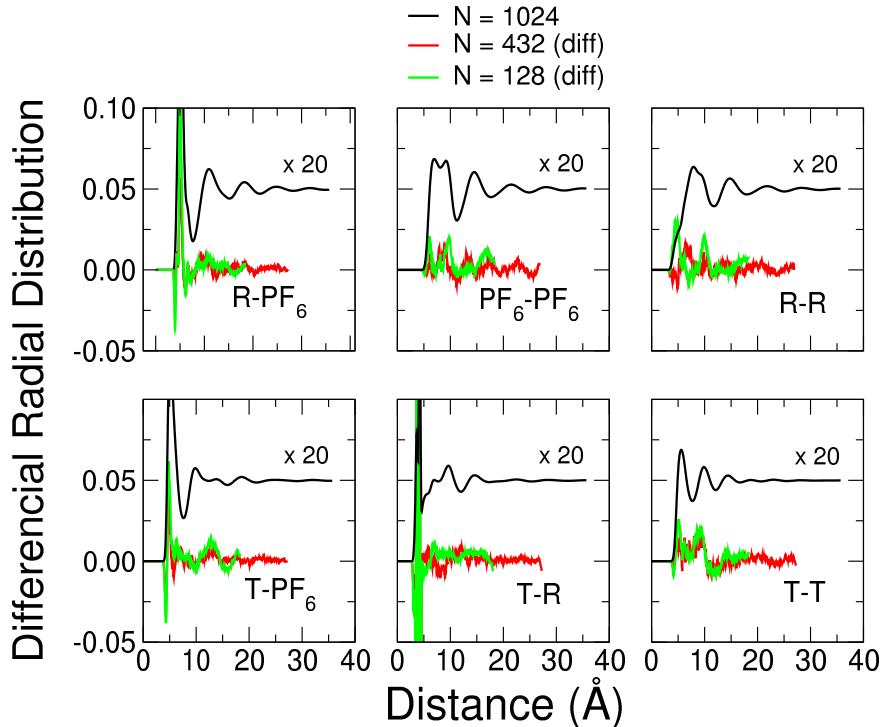


Figure 6. Radial distribution function of the BMIM- PF_6 RTIL, as computed by classical NVT molecular dynamics simulations at 400 K on periodic cell of 128, 432 and 1024 ion pairs using the LHW2004 force field. The BMIM cation is divided in two distinct subregions, corresponding to the charged aromatic ring (R) and the long alkylic tail (T) (see Figure 1). While correlations involving non charged tails disappear for distances as low as 20 angstroms, the radial distribution functions of the larger system (black curves, scaled by a factor of twenty) show that charge induced ordering is negligible only for distances beyond 35 Å. The difference between the radial distribution function computed on the larger system and the ones obtained with smaller cells are reported in green (red) for the 128 (432) ion pairs systems. Despite the fact that, in the smaller systems, correlation lengths are larger than half of the cell sizes, no significant changes in the radial distribution functions are found.

show that system size affects only marginally the computed densities. On the other hand, transport properties tend to show more pronounced changes in going from the smallest to the largest systems. At the lowest temperature considered (300 K), these differences can be attributed to the very slow non ergodic dynamics of the system and to the lack of a true diffusive regime. At the highest temperatures, simulations seems to identify the intermediate size system ($N=432$) as the least mobile one. Nonetheless, size effects have the same order

Systems	T (K)	ρ (g/cm ³)	D^+ (m ² /s)	D^- (m ² /s)	η (mPa s)	λ (S/cm)
$N = 128$	300	1.36	$4.8 \pm 1.0 \cdot 10^{-13}$	$2.6 \pm 0.5 \cdot 10^{-13}$	2400 ± 2000	$1.5 \pm 0.7 \cdot 10^{-4}$
$N = 432$	300	1.36	$1.3 \cdot 10^{-13}$	$5.0 \cdot 10^{-14}$	10000	$2.8 \cdot 10^{-5}$
$N = 1024$	300	1.37	$4.4 \cdot 10^{-13}$	$4.0 \cdot 10^{-13}$	1700	$1.5 \cdot 10^{-4}$
$N = 128$	400	1.29	$3.1 \pm 0.1 \cdot 10^{-11}$	$2.0 \pm 0.3 \cdot 10^{-11}$	111 ± 4	$8.7 \pm 0.6 \cdot 10^{-3}$
$N = 432$	400	1.295	$2.4 \cdot 10^{-11}$	$1.5 \cdot 10^{-11}$	150	$4.2 \cdot 10^{-3}$
$N = 1024$	400	1.297	$3.0 \cdot 10^{-11}$	$2.0 \cdot 10^{-11}$	135	$4.7 \cdot 10^{-3}$
$N = 128$	500	1.22	$2.5 \pm 0.2 \cdot 10^{-10}$	$1.9 \pm 0.1 \cdot 10^{-10}$	12 ± 1	$4.8 \pm 1 \cdot 10^{-2}$
$N = 432$	500	1.222	$2.5 \cdot 10^{-10}$	$1.9 \cdot 10^{-10}$	73	$2.4 \cdot 10^{-2}$
$N = 1024$	500	1.223	$2.9 \cdot 10^{-10}$	$2.3 \cdot 10^{-10}$	37	$4.2 \cdot 10^{-2}$

Table II. Densities ρ , cation diffusion coefficients D^+ , anion diffusion coefficients D^- , viscosities η , and conductivities λ of the BMIM-PF6 RTIL as a function of temperature and system size, as computed by classical NVT molecular dynamics simulations using the LHW2004 force field.

of magnitude as the uncertainty in the computed results and values obtained already on the smaller systems give reasonable estimates of transport properties.

3. Effect of the force field

In order to characterize the effect of the computational parameters on the calculated transport properties of the system, a comparison between different available force fields was performed. In addition to the results discussed in the previous sections, simulations with the interaction potentials developed by Lopes et al. (Ref. [41, 42], in the following abbreviated in CLDP2004), and by Morrow and Maginn (Ref. [23], in the following abbreviated in MM2002), were performed. The differences between these force fields lie mostly in the magnitude of the electrostatic charges and in the description of the four-body bonded interaction (dihedral angles) between the atoms in the ring and the alkyl chains.

In addition, a few test simulations on the CLDP2004 force field have been performed by changing the descriptions of the intramolecular bonds. A set of simulations with the harmonic constants of bonds and angles reduced by half is reported, together with results obtained by constraining all the bond lengths of the system to their equilibrium values.

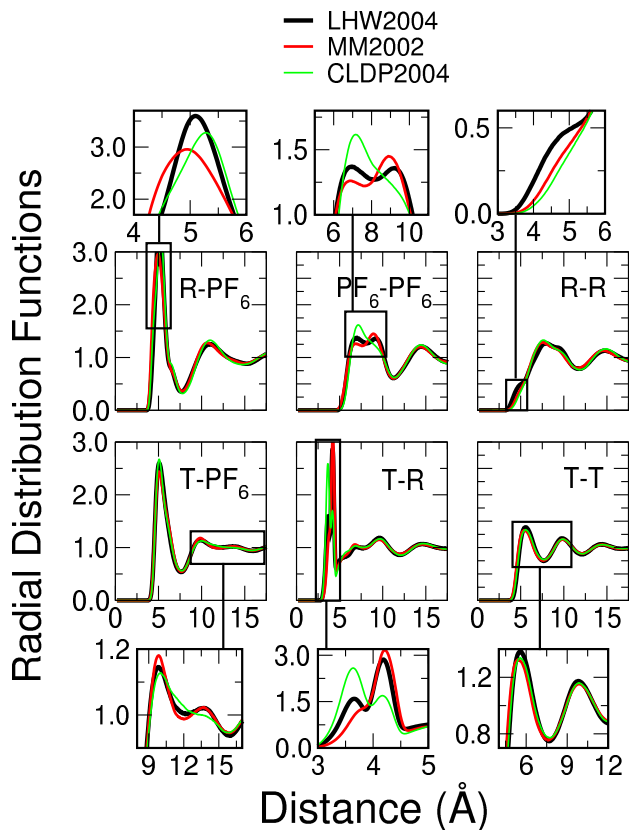


Figure 7. Radial distribution function of the BMIM-PF₆ RTIL, as computed by classical NVT molecular dynamics simulations at 400 K on periodic cell of 128 ion pairs with different force fields. The BMIM cation is partitioned in two distinct subregions, corresponding to the charged aromatic ring (R) and the long alkylic tail (T) (see Figure 1). For each plot, the regions where the radial distribution functions present the largest dependence on the interaction potential have been highlighted in the insets. While most of the radial distributions show only minor differences due to the choice of the force field, the anion-anion distribution function and the intramolecular ring-tail coordination show marked changes in the different simulations. Moreover, only one of the considered force fields shows the appearance of a shoulder at short distances in the ring-ring distribution function.

For all the reported force fields, computed densities are close to the experimental results. On the contrary, radial distribution functions show a marked dependence on the adopted force-field (See Figure 7). The strongest effect of the force field is on the intramolecular ring-tail and the intermolecular anion-anion distribution functions. In the more flexible molecules, the alkyl chain is able to come in closer contact with the ring, thus creating

Systems	T (K)	ρ (g/cm ³)	D^+ (m ² /s)	D^- (m ² /s)	η (mPa s)	λ (S/cm)
LHW2004	300	1.36	$4.8 \pm 1.0 \cdot 10^{-13}$	$2.6 \pm 0.5 \cdot 10^{-13}$	2400 ± 2000	$1.5 \pm 0.7 \cdot 10^{-4}$
MM2002	300	1.353	$3.2 \cdot 10^{-12}$	$2.1 \cdot 10^{-12}$	2200	$4.1 \cdot 10^{-4}$
CLDP2004	300	1.357	$5.0 \cdot 10^{-13}$	$2.1 \cdot 10^{-13}$	7600	$2.3 \cdot 10^{-5}$
LHW2004	350	1.33	$4.0 \pm 1.0 \cdot 10^{-12}$	$2.0 \pm 0.8 \cdot 10^{-12}$	940 ± 400	$1.9 \pm 0.8 \cdot 10^{-3}$
MM2002	350	1.305	$1.3 \cdot 10^{-11}$	$9.4 \cdot 10^{-12}$	77	$3.9 \cdot 10^{-3}$
CLDP2004	350	1.318	$4.2 \cdot 10^{-12}$	$2.3 \cdot 10^{-12}$	903	$7.6 \cdot 10^{-4}$
LHW2004	400	1.29	$3.1 \pm 0.1 \cdot 10^{-11}$	$2.0 \pm 0.3 \cdot 10^{-11}$	111 ± 4	$8.7 \pm 0.6 \cdot 10^{-3}$
MM2002	400	1.268	$8.0 \cdot 10^{-11}$	$5.7 \cdot 10^{-11}$	26	$9.8 \cdot 10^{-3}$
CLDP2004	400	1.275	$2.5 \cdot 10^{-11}$	$1.7 \cdot 10^{-11}$	196	$7.4 \cdot 10^{-3}$
LHW2004	500	1.22	$2.5 \pm 0.2 \cdot 10^{-10}$	$1.9 \pm 0.1 \cdot 10^{-10}$	12 ± 1	$4.8 \pm 1.0 \cdot 10^{-2}$
MM2002	500	1.185	$4.7 \cdot 10^{-10}$	$4.0 \cdot 10^{-10}$	10	$6.1 \cdot 10^{-2}$
CLDP2004	500	1.200	$2.4 \cdot 10^{-10}$	$2.1 \cdot 10^{-10}$	12	$2.7 \cdot 10^{-2}$

Table III. Densities ρ , cation diffusion coefficients D^+ , anion diffusion coefficients D^- , viscosities η , and conductivities λ of the BMIM-PF₆ RTIL as a function of temperature and interaction potentials, as computed by classical NVT molecular dynamics simulations on a system composed by 128 ion pairs.

some steric hindrance that interferes with the cation-anion interactions. This is reflected in the decrease of the second anion-anion peak, together with the slight increase of the mean cation-anion separation.

The effect of constraining all the bonds in the molecule is negligible compared to the other parameters in the interaction potentials. On the contrary, relaxing the force constants of bond and angles is responsible for noticeable changes in the local structures of the liquid, increasing the overall correlation and allowing the charged residues to come in closer contact, at the expense of the non-polar portions of the cations.

Transport properties reflect what was found on the structure of the liquid. In particular, the MM2002 potential shows significantly higher mobility with respect to the other force fields considered. This is probably related to the reduced flexibility of the ring-tail dihedral angle of the cation, that favors an unfolded configuration for the alkyl chain and broadens the cation-anion correlation function. Despite the differences between the LHW2004 and

Systems	T (K)	ρ (g/cm ³)	D^+ (m ² /s)	D^- (m ² /s)	η (mPa s)	λ (S/cm)
CLDP2004	300	1.357	$5.0 \cdot 10^{-13}$	$2.1 \cdot 10^{-13}$	7600	$2.3 \cdot 10^{-5}$
CLDP2004 Rigid	300	1.358	$2.8 \cdot 10^{-13}$	$2.3 \cdot 10^{-13}$	8600	$1.2 \cdot 10^{-4}$
CLDP2004 Flexible	300	1.346	$7.0 \cdot 10^{-13}$	$6.0 \cdot 10^{-13}$	600	$1.4 \cdot 10^{-4}$
CLDP2004	350	1.318	$4.2 \cdot 10^{-12}$	$2.3 \cdot 10^{-12}$	903	$7.6 \cdot 10^{-4}$
CLDP2004 Rigid	350	1.318	$3.7 \cdot 10^{-12}$	$1.9 \cdot 10^{-12}$	474	$7.5 \cdot 10^{-4}$
CLDP2004 Flexible	350	1.314	$5.1 \cdot 10^{-12}$	$2.0 \cdot 10^{-12}$	209	$1.6 \cdot 10^{-3}$
CLDP2004	400	1.275	$2.5 \cdot 10^{-11}$	$1.7 \cdot 10^{-11}$	196	$7.4 \cdot 10^{-3}$
CLDP2004 Rigid	400	1.280	$3.3 \cdot 10^{-11}$	$2.0 \cdot 10^{-11}$	46	$6.5 \cdot 10^{-3}$
CLDP2004 Flexible	400	1.274	$3.5 \cdot 10^{-11}$	$2.3 \cdot 10^{-11}$	69	$9.2 \cdot 10^{-3}$
CLDP2004	500	1.200	$2.4 \cdot 10^{-10}$	$2.1 \cdot 10^{-10}$	12	$2.7 \cdot 10^{-2}$
CLDP2004 Rigid	500	1.203	$2.6 \cdot 10^{-10}$	$2.0 \cdot 10^{-10}$	28	$2.7 \cdot 10^{-2}$
CLDP2004 Flexible	500	1.196	$2.5 \cdot 10^{-10}$	$2.0 \cdot 10^{-10}$	22	$5.0 \cdot 10^{-2}$

Table IV. Densities ρ , cation diffusion coefficients D^+ , anion diffusion coefficients D^- , viscosities η , and conductivities λ of the BMIM-PF₆ RTIL as a function of temperature, as computed by classical NVT molecular dynamics simulations on a system composed by 128 ion pairs and described with the CLDP2004 interaction potential. Different choices of the strength of bonds and angles have been adopted, corresponding to: a) the one reported in the original paper [41, 42]; b) an interaction potential with all the bonds constrained to their equilibrium positions (CLDP2004 Rigid); c) an interaction potential with all the harmonic constants of bonds and angles reduced by half (CLDP2004 Flexible).

the CLDP2004 force fields, diffusion coefficients for the two cases are in close agreement and almost one order of magnitude larger than the experiments. Viscosities and ionic conductivities show a less clear trend with respect to the force field, probably due to the uncertainty in the computed results due to a lack of a proper ensemble averages. Nonetheless, the qualitative picture is consistent with the results of the diffusion coefficients, with MM2002 showing lower viscosities and higher conductivities at all temperatures with respect to the other two force fields. Artificially reducing or increasing the rigidity of the bonds and angles of the CLDP2004 force field has a limited impact on transport properties, the overall effect being within the numerical accuracy of the reported quantities. Contrary to what was found

above for the different classes of force-fields, increasing the overall flexibility of the cation seems to increase the overall diffusivities in the system.

B. Effect of the anion

Three of the most studied anions in RTILs have been considered, namely the PF_6^- , BF_4^- and Tf_2N^- anions. In order to treat all the systems on similar footings, force fields developed by the same group of authors (Lopes et al., Refs. [41, 42] and [43]) were chosen for all the ions. In examining the radial distribution functions, we can see that the two inorganic anions show very similar behavior, with almost identical first peak positions. This reflects the comparable size of the two anions and the similar interactions in the two systems between the fluorine atoms of the anions and the cation. On the contrary, the larger and more asymmetric Tf_2N^- anion presents correlations between charged residues that are broader and shifted towards larger distances. As expected, the cation-cation distribution functions are the least affected by the choice of anion, in particular in the short-ranged tail-tail interactions.

Densities are in good qualitative agreement with experimental results at room temperature, but quantitative results are obtained only for the BMIM- PF_6 system. The other two salts show deviations from experiments much larger than the experimental uncertainty in the data. Similarly to what was obtained for the BMIM- PF_6 RTIL, transport properties of the liquids are within one order of magnitude from corresponding experimental data. Nonetheless, also in this case, computed results show a general good qualitative agreement with experiments at room temperature. The Tf_2N salt is the one showing the highest conductivity and diffusivity and lowest viscosity at room temperature. The PF_6 anion instead is the one giving rise to the least diffusive behavior among the liquids in the whole temperature range considered. It is interesting to notice that, although computed density changes are uniform for the three liquids and linear with temperature, transport properties show temperature dependencies strongly related to the choice of the anion. In particular, the Tf_2N anion is the one showing the smallest variations in the considered temperature interval. As a consequence, already at 400 K the BF_4 liquid shows viscosities and conductivities comparable to the organic anion.

Systems	T (K)	ρ (g/cm ³)	D^+ (m ² /s)	D^- (m ² /s)	η (mPa s)	λ (S/cm)
PF ₆ ⁻	300	1.36	$5.0 \cdot 10^{-13}$	$2.1 \cdot 10^{-13}$	7600	$2.3 \cdot 10^{-5}$
BF ₄ ⁻	300	1.28	$1.3 \cdot 10^{-12}$	$9.2 \cdot 10^{-13}$	414	$6.1 \cdot 10^{-4}$
Tf ₂ N ⁻	300	1.50	$2.5 \cdot 10^{-12}$	$1.6 \cdot 10^{-12}$	158	$1.8 \cdot 10^{-3}$
PF ₆ ⁻	350	1.32	$4.2 \cdot 10^{-12}$	$2.3 \cdot 10^{-12}$	903	$7.6 \cdot 10^{-4}$
BF ₄ ⁻	350	1.24	$1.5 \cdot 10^{-11}$	$1.4 \cdot 10^{-11}$	157	$1.7 \cdot 10^{-3}$
Tf ₂ N ⁻	350	1.45	$2.3 \cdot 10^{-11}$	$1.5 \cdot 10^{-11}$	99	$2.2 \cdot 10^{-3}$
PF ₆ ⁻	400	1.28	$2.5 \cdot 10^{-11}$	$1.7 \cdot 10^{-11}$	196	$7.4 \cdot 10^{-3}$
BF ₄ ⁻	400	1.20	$8.5 \cdot 10^{-11}$	$6.8 \cdot 10^{-11}$	39	$8.4 \cdot 10^{-3}$
Tf ₂ N ⁻	400	1.40	$9.7 \cdot 10^{-11}$	$7.3 \cdot 10^{-11}$	40	$1.1 \cdot 10^{-2}$
PF ₆ ⁻	500	1.20	$2.4 \cdot 10^{-10}$	$2.1 \cdot 10^{-10}$	12	$2.7 \cdot 10^{-2}$
BF ₄ ⁻	500	1.13	$4.7 \cdot 10^{-10}$	$4.0 \cdot 10^{-10}$	25	$7.6 \cdot 10^{-2}$
Tf ₂ N ⁻	500	1.32	$3.6 \cdot 10^{-10}$	$3.2 \cdot 10^{-10}$	24	$4.1 \cdot 10^{-2}$

Table V. Densities ρ , cation diffusion coefficients D^+ , anion diffusion coefficients D^- , viscosities η , and conductivities λ of BMIM-based RTILs as a function of temperature, as computed by classical NVT molecular dynamics simulations on a system composed by 128 ion pairs and described with the CLDP2004 interaction potential.

IV. CONCLUSIONS

In summary, a series of extensive classical MD simulations on BMIM based ionic liquids have been reported. A careful analysis of simulation parameters have been performed to estimate the accuracy of the computed results. The highly viscous nature of the ionic liquids studied poses serious problems in evaluating transport properties and was show to require simulation times larger than 100 ns to converge below 400 K. In most cases, converged quantities could only be estimated at room temperature, for which the systems studied are in fact trapped in glass-like dynamics. Diffusion coefficients, viscosities and conductivities all show good qualitative agreement and correct temperature trends when compared with experimental results. The correct trend of the transport properties for the different ionic liquids is recovered, with BMIM-Tf₂N being the less viscous RTIL and BMIM-PF₆ showing the slowest dynamics. Nonetheless, results remain one order of magnitude away

from experimental data. This discrepancy could be due to the neglect of polarizability in the interaction potentials, or due to even small fraction of impurities in the experimental setups.

ACKNOWLEDGMENTS

This work was supported by E. I. du Pont de Nemours & Co. through the DuPont-MIT Alliance program. The authors acknowledge Shyue Ping Ong, Gerbrand Ceder, Steve R. Lustig and William L. Holstein for useful discussions and collaborations.

-
- [1] N. V. Plechkova and K. R. Seddon, *Chemical Society Reviews* **37**, 123 (2008)
 - [2] P. Walden, *Bulletin de l'Academie Imperiale des Sciences de St.Petersbourg* **8**, 405 (1914)
 - [3] J. S. Wilkes and C. L. Hussey, Frank J. Seiler Research Laboratory Technical Report(1982)
 - [4] J. S. Wilkes, J. A. Levisky, R. A. Wilson, and C. L. Hussey, *Inorganic Chemistry* **21**, 1263 (1982)
 - [5] C. L. Hussey, *Pure and Applied Chemistry* **60**, 1763 (1988)
 - [6] A. K. Abdulsada, A. G. Avent, M. J. Parkington, T. A. Ryan, K. R. Seddon, and T. Welton, *Journal of the Chemical Society-Chemical Communications*, 1643(1987)
 - [7] A. K. Abdulsada, A. G. Avent, M. J. Parkington, T. A. Ryan, K. R. Seddon, and T. Welton, *Journal of the Chemical Society-Dalton Transactions*, 3283(1993)
 - [8] J. S. Wilkes and M. J. Zaworotko, *Journal of the Chemical Society-Chemical Communications*, 965(1992)
 - [9] H. Weingärtner, *Angewandte Chemie International Edition* **47**, 654 (2008)
 - [10] K. Binnemans, *Chemical Reviews* **107**, 2592 (2007)
 - [11] J. Dupont, R. F. de Souza, and P. A. Z. Suarez, *Chemical Reviews* **102**, 3667 (2002)
 - [12] T. L. Greaves and C. J. Drummond, *Chemical Reviews* **108**, 206 (2008)
 - [13] P. Hapiot and C. Lagrost, *Chemical Reviews* **108**, 2238 (2008)
 - [14] F. van Rantwijk and R. A. Sheldon, *Chemical Reviews* **107**, 2757 (2007)
 - [15] P. Bonhote, A. P. Dias, M. Armand, N. Papageorgiou, K. Kalyanasundaram, and M. Gratzel, *Inorganic Chemistry* **35**, 1168 (1996)

- [16] S. Ito, S. M. Zakeeruddin, P. Comte, P. Liska, D. B. Kuang, and M. Gratzel, *Nature Photonics* **2**, 693 (2008)
- [17] D. Kuang, S. Uchida, R. Humphry-Baker, S. M. Zakeeruddin, and M. Gratzel, *Angewandte Chemie-International Edition* **47**, 1923 (2008)
- [18] A. Farnicola, S. Panero, B. Scrosati, M. Tamada, and H. Ohno, *Chemphyschem* **8**, 1103 (2007)
- [19] A. Farnicola, F. Croce, B. Scrosati, T. Watanabe, and H. Ohno, *Journal of Power Sources* **174**, 342 (2007)
- [20] K. R. Seddon, A. Stark, and M. J. Torres, *Pure and Applied Chemistry* **72**, 2275 (2000)
- [21] A. L. Rollet, P. Porion, M. Vaultier, I. Billard, M. Deschamps, C. Bessada, and L. Jouvencal, *Journal of Physical Chemistry B* **111**, 11888 (2007)
- [22] C. G. Hanke, S. L. Price, and R. M. Lynden-Bell, *Molecular Physics* **99**, 801 (2001)
- [23] T. I. Morrow and E. J. Maginn, *Journal of Physical Chemistry B* **106**, 12807 (2002)
- [24] J. K. Shah, J. F. Brennecke, and E. J. Maginn, *Green Chemistry* **4**, 112 (2002)
- [25] J. K. Shah and E. J. Maginn, *Fluid Phase Equilibria* **222**, 195 (2004)
- [26] C. J. Margulis, H. A. Stern, and B. J. Berne, *Journal of Physical Chemistry B* **106**, 12017 (2002)
- [27] J. de Andrade, E. S. Boes, and H. Stassen, *Journal of Physical Chemistry B* **106**, 3546 (2002)
- [28] J. de Andrade, E. S. Boes, and H. Stassen, *Journal of Physical Chemistry B* **106**, 13344 (2002)
- [29] P. A. Hunt, *Molecular Simulation* **32**, 1 (2006)
- [30] T. Y. Yan, C. J. Burnham, M. G. Del Popolo, and G. A. Voth, *Journal of Physical Chemistry B* **108**, 11877 (2004)
- [31] Z. H. Hu and C. J. Margulis, *Proceedings of the National Academy of Sciences of the United States of America* **104**, 9546 (2007)
- [32] J. Habasaki and K. L. Ngai, *Journal of Chemical Physics* **129**, 194501 (2008)
- [33] B. Qiao, C. Krekeler, R. Berger, L. Delle Site, and C. Holm, *Journal of Physical Chemistry B* **112**, 1743 (2008)
- [34] C. Cadena, Q. Zhao, R. Q. Snurr, and E. J. Maginn, *Journal of Physical Chemistry B* **110**, 2821 (2006)
- [35] C. Rey-Castro and L. F. Vega, *Journal of Physical Chemistry B* **110**, 14426 (2006)
- [36] C. Rey-Castro and L. F. Vega, *Journal of Physical Chemistry B* **110**, 16157 (2006)
- [37] W. Smith and T. R. Forester, *Journal of Molecular Graphics* **14**, 136 (1996)

- [38] W. Smith, C. W. Yong, and P. M. Rodger, *Molecular Simulation* **28**, 385 (2002)
- [39] W. Smith, *Molecular Simulation* **32**, 933 (2006)
- [40] Z. P. Liu, S. P. Huang, and W. C. Wang, *Journal of Physical Chemistry B* **108**, 12978 (2004)
- [41] J. N. C. Lopes, J. Deschamps, and A. A. H. Padua, *Journal of Physical Chemistry B* **108**, 2038 (2004)
- [42] J. N. C. Lopes, J. Deschamps, and A. A. H. Padua, *Journal of Physical Chemistry B* **108**, 11250 (2004)
- [43] J. N. C. Lopes and A. A. H. Padua, *Journal of Physical Chemistry B* **108**, 16893 (2004)
- [44] H. J. C. Berendsen, J. P. M. Postma, W. F. Vangunsteren, A. Dinola, and J. R. Haak, *Journal of Chemical Physics* **81**, 3684 (1984)
- [45] S. Nose, *Molecular Physics* **52**, 255 (1984)
- [46] W. G. Hoover, *Physical Review A* **31**, 1695 (1985)
- [47] D. Frenkel and B. Smit, *Understanding Molecular Simulation, From Algorithms to Applications*, 2nd ed., Computational Science, From Theory to Applications, Vol. 1 (Academic Press, Inc., 2001)
- [48] M. Allen and D. J. Tildesley, *Computer Simulation of Liquids*, paperback ed. (Oxford University Press, USA, 1989)
- [49] H. Tokuda, K. Hayamizu, K. Ishii, M. Abu Bin Hasan Susan, and M. Watanabe, *Journal of Physical Chemistry B* **108**, 16593 (2004)
- [50] H. Jin, B. O'Hare, J. Dong, S. Arzhantsev, G. A. Baker, J. F. Wishart, A. J. Benesi, and M. Maroncelli, *Journal of Physical Chemistry B* **112**, 81 (2008)
- [51] S. Tsuzuki, W. Shinoda, H. Saito, M. Mikami, H. Tokuda, and M. Watanabe, *Journal of Physical Chemistry B* **113**, 10641 (2009)

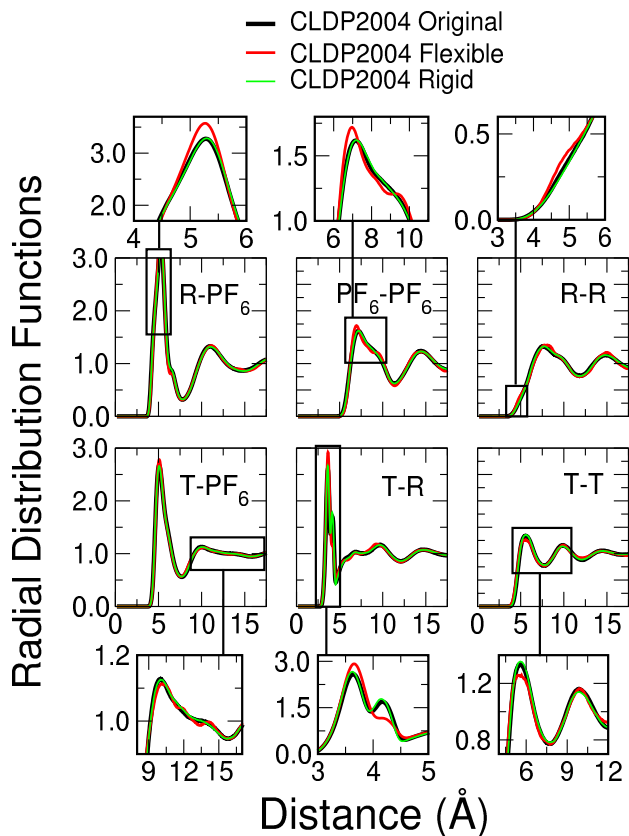


Figure 8. Radial distribution function of the BMIM-PF₆ RTIL, as computed by classical NVT molecular dynamics simulations at 400 K on periodic cell of 128 ion pairs described by the CLDP2004 force field. For each plot, the regions where the radial distribution functions present the largest dependence on the interaction potential have been highlighted in the insets. Different choices of the strength of bonds and angles have been adopted, corresponding to the one reported in the original paper [41, 42] (CLDP2004 Original), to an interaction potential with all the bonds constrained to their equilibrium positions (CLDP2004 Rigid) and to an interaction potential with all the harmonic constants of bonds and angles reduced by half (CLDP Flexible). While the description of the intramolecular bonds appear to affect only marginally the structure of the liquid, increasing the flexibility of the harmonic three body interactions (angles) has a marked effect on the computed distribution functions. In particular, the resulting liquid show a higher correlation between the charged residues at the expenses of the short-ranged tail tail distribution.

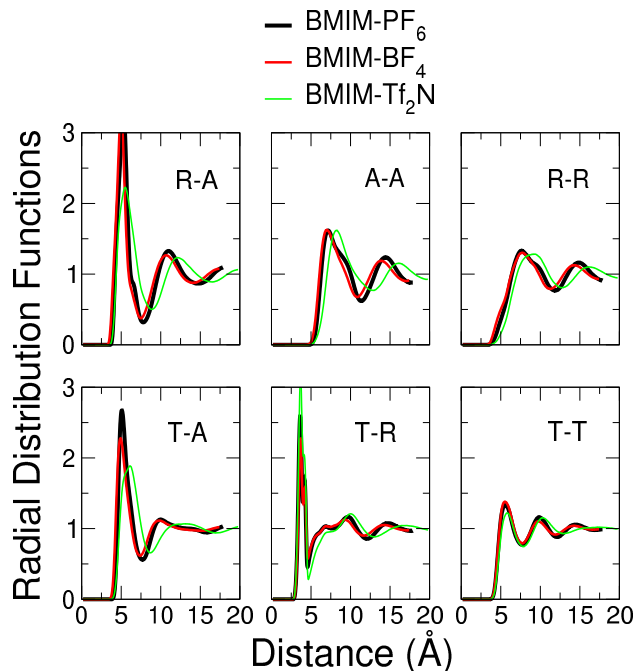


Figure 9. Radial distribution function of BMIM-based RTILs for three different anions as computed by classical NVT molecular dynamics simulations at 400 K on periodic cell of 128 ion pairs described by the CLDP2004 force field. The three anions considered (A) are PF_6^- (thick black line), BF_4^- (red line) and Tf_2N^- (thin green line). The two inorganic anions show very similar distribution functions, with almost identical first peak positions. This reflects the similar interactions in the two systems between the fluorine atoms of the anions and the cation. On the contrary, the larger and more asymmetric Tf_2N^- anion presents correlations between charged residues that are broader and shifted towards larger distances, while the short-ranged tail-tail interactions in the cation are only slightly affected.

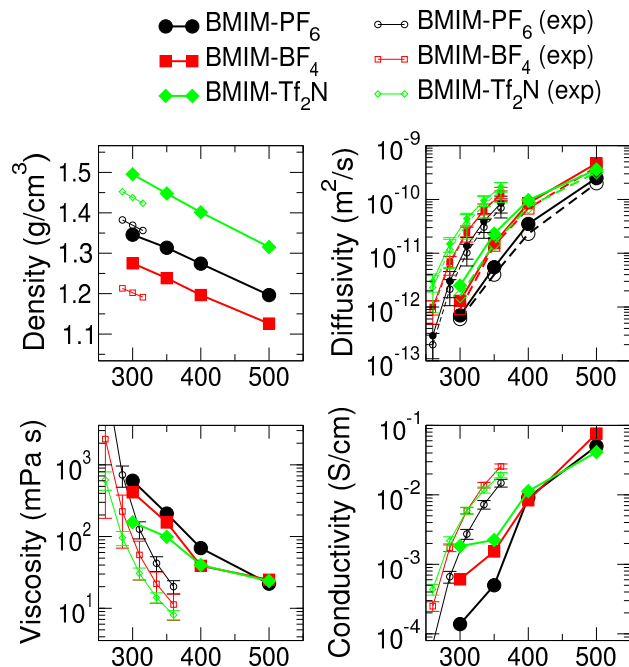


Figure 10. Density, diffusion coefficients for anions (open symbols-dashed lines) and cations (filled symbols-continuous lines), viscosity, and conductivity of BMIM-based ionic liquids for three different anions as computed by classical NVT molecular dynamics simulations at 400 K on a system composed of 128 ion pairs, as described by the CLDP2004 force field. The three anions considered are PF₆⁻ (black circles), BF₄⁻ (red squares) and Tf₂N⁻ (green diamonds). Experimental results from Ref. [49] are also reported for comparison.